

Synthesis, structure and solution dynamics of lithium salts of superbulky cyclopentadienyl ligands

Garth R. Giesbrecht,^{*a} John C. Gordon,^b David L. Clark^c and Brian L. Scott^b

^a Nuclear Materials Technology Division, Los Alamos National Laboratory, Mail Stop J514, Los Alamos, NM 87545. E-mail: garth@lanl.gov

^b Chemistry Division, Los Alamos National Laboratory, Mail Stop J514, Los Alamos, NM 87545

^c Glenn T. Seaborg Institute for Transactinium Science, Los Alamos National Laboratory, Mail Stop E500, Los Alamos, NM 87545

Received 26th February 2003, Accepted 6th May 2003

First published as an Advance Article on the web 27th May 2003

The superbulky cyclopentadienes (CpAr[#])H (Ar[#] = 3,5-Me₂C₆H₃ (**1a**); Ar[#] = 3,5-^tBu₂C₆H₃ (**1b**)) were prepared by the palladium-catalyzed reaction of metallocenes with aryl bromides. NMR spectroscopy was consistent with C_s symmetric solution structures with free rotation of the substituted aryl rings. The molecular structure of **1a** is similar to that previously determined for pentaphenylcyclopentadiene, with a planar Cp ring bisected by an approximate mirror plane. Addition of BuLi to **1a,b** yielded the lithium salts (CpAr[#])Li(THF)₂ (**2a**) and (CpAr[#])Li (**2b**) in good yield. ⁷Li NMR spectroscopy of **2a,b** indicated more than one species in solution. Crystallization of **2a** from toluene revealed an infinite one-dimensional chain structure with alternating [(CpAr[#])₂Li]⁻ and [(THF)Li(CpAr[#])Li(CpAr[#])-Li(THF)]⁺ units; due to the sterics of the Cp rings, the lithium atom appears to be only loosely held in place with a larger than usual Li–Cp distance. ⁷Li NMR spectroscopy suggested an equilibrium between the monomeric species (CpAr[#])Li(THF)_x and the metallate [(CpAr[#])₂Li][Li(THF)_x] in C₆D₆ which was supported by variable temperature and NOESY ⁷Li NMR experiments. Crystallization of **2a** from THF/TMEDA yielded the solvent separated ion pair [(CpAr[#])₂Li][Li(TMEDA)₂] (**3a**). In this case, ⁷Li NMR spectroscopy pointed towards the presence of a single species in solution.

Introduction

The cyclopentadienide anion and its many variants are among the most common ligands in organometallic chemistry.¹ Replacement of the hydrogen atoms of the C₅H₅ ligand with alkyl, silyl or aryl groups provides the opportunity to systematically alter the electronic and steric properties of the ligand, which directly influence the chemical properties of the resultant metal complexes. A well known approach to the kinetic stabilization of thermodynamically unstable compounds is the use of large ancillary ligands. Unfortunately, the utilization of “superbulky” cyclopentadienyl derivatives has often been hampered by arduous, multi-step synthetic procedures.^{2,3} Recent advances in this area have made such target molecules more accessible^{4,5} and have already proven useful in the synthesis of new catalysts for a number of enantioselective transformations.⁶

The structures of organolithium complexes in solution have been the focus of much attention, due to the unique manner in which the lithium center can interact with the organic moiety. Extensive studies on enolates⁷ and lithium amide bases^{8,9} have revealed a complex solution behavior, with numerous dynamic processes and unusual solution structures being proposed. For example, CpLi exists as a triple ion below –100 °C, with an equilibrium between monomeric LiCp and a metallate-type complex.¹⁰ The inherently fast rate of this exchange may be slowed down by employing bulkier cyclopentadienyl groups. Thus, with sterically encumbered ligands such as isodicyclopentadienide,¹⁰ it is possible to structurally characterize both

members of this equilibrium by the addition of the appropriate Lewis base.¹¹ In this manner, one can gain further insight into structural motifs postulated to occur in solution, but only indirectly observed previously by methods such as NMR spectroscopy. We present here the synthesis and characterization of lithium salts of two superbulky cyclopentadienyl ligands, the effect of the addition of different Lewis bases, and the properties of these complexes in solution.

Results and discussion

Synthesis of (CpAr[#])H (Ar[#] = 3,5-Me₂C₆H₃ (**1a**); Ar[#] = 3,5-^tBu₂C₆H₃ (**1b**))

The preparation of superbulky cyclopentadienyl derivatives was accomplished according to the methodology developed by Dyker and Muira *via* the multiple arylation of metallocenes with aryl bromides in palladium-catalyzed reactions [eqn. (1)].^{4,5} The dimethylphenyl derivative (CpAr[#])H (Ar[#] = 3,5-Me₂C₆H₃) (**1a**) has been previously reported⁵ and has been successfully utilized as a supporting ligand for a new class of asymmetric catalysts.⁶ The bulkier di-*tert*-butylphenyl analogue (CpAr[#])H (Ar[#] = 3,5-^tBu₂C₆H₃) (**1b**) was synthesized in a similar fashion in good yield. The *tert*-butyl derivative is more soluble in hydrocarbon solvents than the dimethyl version, being soluble in solvents such as hexane and diethyl ether. Both compounds may be isolated as pale yellow powders following workup. The cyclopentadienes **1a,b** are C_s symmetric as

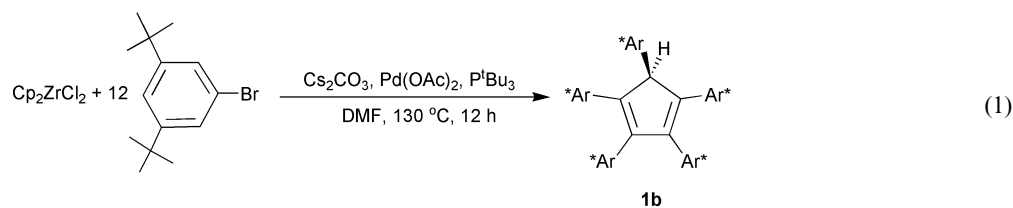


Table 1 Selected bond distances (Å) and angles (°) for (CpAr[#])₅H (**1a**) (Ar[#] = 3,5-Me₂C₆H₃)

C1–C2	1.504(4)	C2–C3	1.348(4)
C3–C4	1.471(4)	C4–C5	1.337(4)
C5–C1	1.508(4)	C1–C6	1.516(4)
C2–C14	1.472(4)	C3–C22	1.481(4)
C4–C30	1.485(4)	C5–C38	1.472(4)
C2–C1–C5	103.2(2)	C2–C1–C6	112.9(2)
C5–C1–C6	111.0(2)	C1–C2–C3	108.7(3)
C1–C2–C14	122.6(3)	C3–C2–C14	128.6(3)
C2–C3–C4	109.4(3)	C2–C3–C22	127.3(3)
C4–C3–C22	123.1(3)	C3–C4–C5	109.2(3)
C3–C4–C30	123.1(3)	C5–C4–C30	127.7(3)
C4–C5–C1	109.3(3)	C4–C5–C38	128.8(3)
C1–C5–C38	121.7(3)		

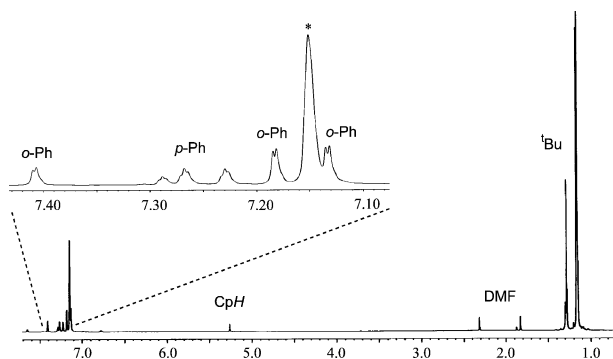


Fig. 1 500 MHz ¹H NMR spectrum of (CpAr^{*})₅H (**1b**) (Ar^{*} = 3,5-^tBu₂C₆H₃) in C₆D₆. * denotes residual solvent.

indicated by their ¹H NMR spectra; the ¹H NMR spectrum of **1b** is shown in Fig. 1. The *tert*-butyl resonances appear as singlets at 1.28, 1.16 and 1.15 ppm in an 18 : 36 : 36 ratio, reflecting the three distinct types of phenyl rings present in **1b**. This intensity ratio is mirrored in the aromatic region of the spectrum where the *para*-protons of the phenyl rings appear as triplets in a 1 : 2 : 2 ratio (7.29, 7.27, 7.23 ppm; ⁴J_{H–H} = 1.5 Hz) and the *ortho*-protons are evidenced by doublets of 2 : 4 : 4 intensity at 7.41, 7.18 and 7.13 ppm. The CpH proton is observed as a singlet at 5.24 ppm. In spite of the fact that the molecule has two distinct sides, due to the presence of the sp³ carbon of the cyclopentadiene ring, only three sets of phenyl resonances are observed, indicating that even with the extremely bulky *di-tert*-butylphenyl group, free rotation is still possible. In contrast, *ortho*-substituted derivatives such as penta(2,5-dimethylphenyl)-cyclopentadiene consist of at least six rotamers in solution at room temperature due to restricted movement of two adjacent methyl groups which makes the rotation of the phenyl groups difficult.⁵ It is difficult to remove residual DMF (DMF = dimethylformamide) from compound **1b**; even after prolonged exposure to vacuum, the ¹H NMR spectrum shows resonances for DMF (see Fig. 1). Also, the elemental analysis of **1b** is consistent with the presence of one DMF molecule per cyclopentadiene unit (see Experimental).

Molecular structure of (CpAr[#])₅H (**1a**) (Ar[#] = 3,5-Me₂C₆H₃)

Crystals of **1a** that were suitable for an X-ray diffraction study were grown by slow evaporation of a concentrated toluene solution. Selected bond lengths and angles are presented in Table 1. A thermal ellipsoid plot giving the atom-numbering scheme used in the tables is shown in Fig. 2a; complete details of the structural analyses of compounds **1a**, **2a** and **3a** are listed in Table 4. The solid state structure consists of a planar cyclopentadiene ring which is bisected by an approximate mirror plane, containing the unique phenyl ring, the sp³ carbon atom and the unique hydrogen atom. The structure is similar to that previously determined for pentaphenylcyclopentadiene.¹² The C–C–C angles of the alkenyl carbons of the Cp ring are ~109°,

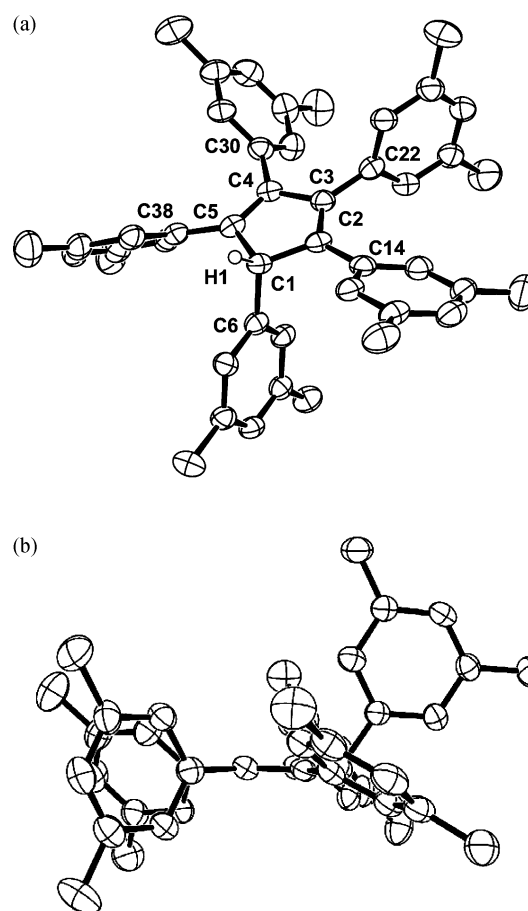
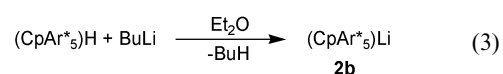
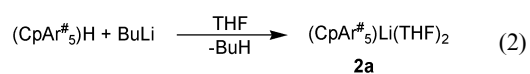


Fig. 2 (a) Thermal ellipsoid view of (CpAr[#])₅H (**1a**) (Ar[#] = 3,5-Me₂C₆H₃) drawn with 30% probability ellipsoids, giving the atom numbering scheme used in the tables. (b) Side view of (CpAr[#])₅H (**1a**) drawn with 30% probability ellipsoids.

while the corresponding angle at the sp³-hybridized carbon (C1) is 103.2(2)°. The average of the C–C bond lengths in the Cp ring is 1.434(4) Å, which is similar to that found in pentaphenylcyclopentadiene (1.443 Å).¹² The two bonds to the tetrahedral carbon are longer than the other ring C–C bonds (1.504(4) and 1.508(4) Å), as is observed in pentaphenylcyclopentadiene¹² and tetraphenylcyclopentadiene.¹³ The Cp ring is planar to within 0.0125 Å, with the *ipso*-carbons of the alkenyl substituted phenyl rings located out of the Cp plane by 0.0206–0.0720 Å (Fig. 2b). The *ipso*-carbon of the remaining phenyl ring lies 1.255 Å out of the plane of the Cp ring. The phenyl rings are canted at angles of 33.1, 90.9, 55.2 and 52.4° with respect to the Cp ring (57.9° (ave)). These values compare with those previously observed for similar complexes (*i.e.* the four alkenyl phenyl rings in pentaphenylcyclopentadiene are canted an average of 49.7°).¹² The slightly larger value for **1a** is likely a reflection of the larger steric bulk of the 3,5-dimethylphenyl analogue.

Synthesis of lithium salts (CpAr[#])₅Li (Ar[#] = 3,5-Me₂C₆H₃; Ar^{*} = 3,5-^tBu₂C₆H₃)

The addition of BuLi to solutions of (CpAr[#])₅H (**1a**) or (CpAr^{*})₅H (**1b**) resulted in the formation of the lithium salts (CpAr[#])₅Li(THF)₂ (**2a**) (THF = tetrahydrofuran) and (CpAr[#])₅Li (**2b**) in good yield [eqns. (2) and (3)].



Deprotonation of the dimethylphenyl derivative **1a** was performed in THF (the starting cyclopentadiene has only limited solubility in diethyl ether), yielding the lithium salt **2a** as a yellow solid. Compound **2a** is somewhat soluble in toluene and THF and the ^1H NMR spectrum (C_6D_6) indicates approximately two coordinated molecules of THF per lithium center. Exposure to vacuum results in removal of some of the coordinated THF, which is further supported by the elemental analysis of **2a**, which corresponds to a formulation of 1.5 THF molecules for every metal center. The ^1H and ^{13}C NMR spectra of **2a** were complicated by the presence of additional peaks due to other lithium containing species; the nature of these species was elucidated by ^7Li NMR studies and will be discussed later. However, NMR spectroscopy indicates that the major product upon workup is the monomeric species, $(\text{CpAr}^\#)_2\text{Li}(\text{THF})_2$. The larger cyclopentadiene **1b** reacts similarly with BuLi in diethyl ether to yield the base-free complex $(\text{CpAr}^\#)_2\text{Li}$ as a colorless solid; in this case there was no evidence for the presence of coordinated Lewis base, likely as a result of the more crowded coordination sphere around the lithium center in the di-*tert*-butylphenyl derivative. Also, ^1H and ^{13}C NMR spectroscopy of **2b** were consistent with a single product in solution. The aryl region exhibited two peaks in a 2 : 1 ratio due to the *ortho* and *para*-protons of the 3,5- $^t\text{Bu}_2\text{C}_6\text{H}_3$ rings; these peaks appear as a broad doublet and triplet, respectively ($^4J_{\text{H-H}} = 1.5$ Hz). As is the case for the cyclopentadiene **1b**, in spite of the asymmetry in the molecule, a single doublet is observed for the *ortho*-protons, indicating rapid rotation of the bulky di-*t*-butyl-phenyl rings. Interestingly, the analogous resonances for the smaller dimethyl analogue **2a** are broad singlets, suggesting that the rate of rotation of these substituted phenyl rings is slower, and perhaps dependent on other steric factors, such as aggregation or metallate formation in solution. Although the ^1H and ^{13}C NMR spectra of **2b** were consistent with a single species in solution, ^7Li revealed the presence of more than one compound; this feature of the solution behavior of **2b** will be discussed later.

A persistent problem encountered when handling solutions of the lithium salts was the gradual appearance of a dark blue or violet contaminant which we attribute to the formation of the penta-arylated cyclopentadienyl radicals, CpAr_5^\cdot .¹⁴ We found these radicals to rapidly react with THF to generate the starting cyclopentadienes. Thus, it was important to handle the lithium salts either in the absence of THF or for very short periods when necessary. This tendency was more pronounced with the di-*tert*-butylphenyl species **2b**; for this reason, the lithium salt was synthesized using diethyl ether as the reaction solvent. However, the low solubility of the dimethylphenyl analogue in diethyl ether necessitated the use of THF for the lithiation reaction. We cannot rule out the possibility that the ether adduct $(\text{CpAr}^\#)_2\text{Li}(\text{ether})_x$ is formed in solution also. We were not able to obtain X-ray quality crystals of $(\text{CpAr}^\#)_2\text{Li}$ or its ether adduct; thus we focused our attention on the less soluble 3,5-dimethylphenyl derivative.

Molecular structures of $\{[(\text{CpAr}^\#)_2\text{Li}][\text{Li}(\text{THF})(\text{THF})]_x\}$ (**2a**) and $[(\text{CpAr}^\#)_2\text{Li}][\text{Li}(\text{TMEDA})_2]$ (**3a**) ($\text{Ar}^\# = 3,5\text{-Me}_2\text{C}_6\text{H}_3$)

Colorless crystals of **2a** that were amenable to X-ray diffraction studies were grown by slow evaporation of a saturated toluene solution. A thermal ellipsoid diagram of the repeat unit is shown in Fig. 3; important bond lengths and angles are given in Table 2. The molecule co-crystallizes with one molecule of THF in the lattice. The two cyclopentadienyl rings within each $[(\text{CpAr}^\#)_2\text{Li}]^-$ unit are related by symmetry, and thus Table 2 contains only bond lengths between the lithium center and one of the Cp groups. The solid state structure consists of an infinite one-dimensional chain with alternating $[(\text{CpAr}^\#)_2\text{Li}]^-$ and $[(\text{THF})\text{Li}(\text{CpAr}^\#)_2\text{Li}(\text{CpAr}^\#)_2\text{Li}(\text{THF})]^+$ units (Fig. 4). This extended chain structure is similar to that determined for CpM ($\text{M} = \text{Li}, \text{Na}, \text{K}$)¹⁵ or $(1,2,4\text{-}(\text{SiMe}_3)_3\text{Cp})\text{K}$ ¹⁶ and is a common

Table 2 Selected bond distances (Å) and angles (°) for $\{[(\text{CpAr}^\#)_2\text{Li}][\text{Li}(\text{THF})(\text{THF})]_x\}$ (**2a**) ($\text{Ar}^\# = 3,5\text{-Me}_2\text{C}_6\text{H}_3$)^a

Li1–Cp1	2.094	Li1–C1	2.444(5)
Li1–C2	2.438(5)	Li1–C3	2.431(5)
Li1–C4	2.403(5)	Li1–C5	2.397(5)
Li2–Cp1	1.866	Li2–C1	2.18(2)
Li2–C2	2.23(2)	Li2–C3	2.28(2)
Li2–C4	2.27(2)	Li2–C5	2.21(2)
Li2–O1	1.80(2)	Li2'–C93	1.99(2)
Li2'–C94	2.23(2)	Cp1–Li1–Cp1*	180.00
Li1–Cp1–Li2	176.79	Cp1–Li2–O1	177.49

^a Cp1 is defined as the centroid arising from atoms C1 – C5; Cp1* is related to Cp1 by symmetry. The ' designation refers to one of two disordered sites for Li2.

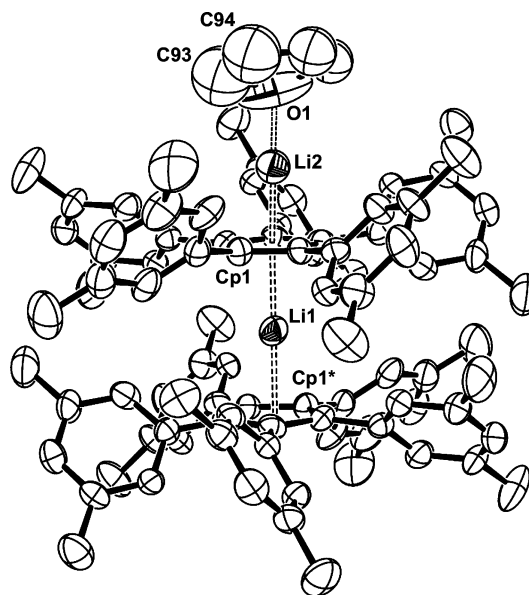


Fig. 3 Thermal ellipsoid view of the repeat unit of $\{[(\text{CpAr}^\#)_2\text{Li}][\text{Li}(\text{THF})(\text{THF})]_x\}$ (**2a**) ($\text{Ar}^\# = 3,5\text{-Me}_2\text{C}_6\text{H}_3$) drawn with 30% probability ellipsoids, giving the atom numbering scheme used in the tables. An interstitial molecule of THF is omitted for clarity. Cp1 is defined as the centroid arising from atoms C1–C5; Cp1* is defined as the centroid arising from atoms C1*–C5*. For the sake of clarity, only the centroid designations are given. Only one of the two disordered Li2 sites is shown.

motif in alkali metal cyclopentadienides. However, solvated alkali metal cyclopentadienides such as $[(\text{THF})\text{K}(\mu\text{-C}_5\text{Me}_5)]_x$ ¹⁷ or $[(\text{DME})\text{Na}(\mu\text{-C}_5\text{H}_5)]_x$ ¹⁸ ($\text{DME} = \text{dimethoxyethane}$) exhibit solid state structures in which the metal atom is sandwiched between two Cp rings, with the alkali metal coordinated by the Lewis base. In the case of **2a**, the steric bulk of the 3,5- $\text{Me}_2\text{C}_6\text{H}_3$ groups apparently prevents such an arrangement from being obtained. As observed in Fig. 3, the $(\text{CpAr}^\#)_2\text{Li}_2(\text{THF})$ unit contains two substituted Cp rings which are planar to each other, in order to minimize steric repulsion. If Li1 were to coordinate a molecule of THF, a bent structure would likely result, as seen for $[(\text{THF})\text{K}(\mu\text{-C}_5\text{Me}_5)]_x$ or $[(\text{THF})_2\text{K}(\mu\text{-C}_5\text{Me}_5)]_x$. The large size of the penta-arylated cyclopentadienyl rings makes this bent arrangement unfavorable. Thus, the exogenous lithium atom (Li2), which is bound to a single Cp ring, coordinates to the THF molecule. Li2 is disordered equally over two sites; for the sake of clarity only one orientation is shown. In addition to the position shown in Figs. 3 and 4, Li2 also occupies the vacancy between the THF of the $[(\text{THF})\text{Li}(\text{CpAr}^\#)_2\text{Li}(\text{CpAr}^\#)_2\text{Li}(\text{THF})]^+$ units and the Cp ring of the $[(\text{CpAr}^\#)_2\text{Li}]^-$ groups. In this case, the lithium ion coordinates to the cyclopentadienyl ring and makes close contact with two carbon atoms of the THF molecule ($\text{Li2}'\text{-C93} = 1.99(2)$ Å, $\text{Li2}'\text{-C94} = 2.23(2)$ Å). It is the combination of these two disordered lithium sites that is responsible for the

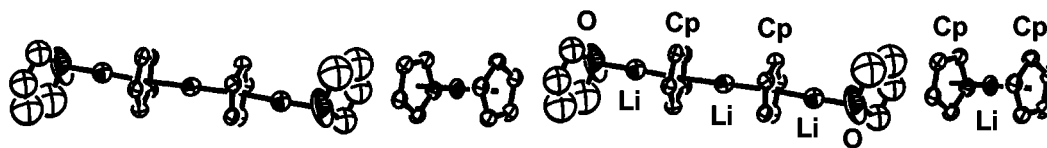


Fig. 4 Thermal ellipsoid view of the one-dimensional chain structure of $\{[(\text{CpAr}^\#)_2\text{Li}][\text{Li}(\text{THF})](\text{THF})_x\}_n$ (**2a**) ($\text{Ar}^\# = 3,5\text{-Me}_2\text{C}_6\text{H}_3$) drawn with 30% probability ellipsoids. 3,5-dimethylphenyl rings omitted for clarity. Only one of the two disordered Li2 sites is shown.

long range structure of **2a**. The lithium atom that is sandwiched between two Cp rings is only loosely held in place, as seen by the large Li1–Cp1 distances of 2.094 Å. This is significantly longer than the distance of 1.969 Å observed in polymeric LiCp ,¹⁵ or distances of 2.03 and 1.78 Å for $\{[\text{Li}(\eta^5\text{-C}_5\text{Bz}_5)]_2(\text{C}_6\text{D}_6)\}$ (Bz = benzyl).¹⁹ The Li1–C distances range from 2.397(5)–2.444(5) Å; these larger than normal distances are the likely result of the steric demands of the 3,5-Me₂C₆H₃ rings. The substituted phenyl rings are canted an average of 48.6° with respect to the cyclopentadienyl groups for both rings, although in opposite directions, resulting in a “gear-meshing” and a closer approach of the two Cp rings. In contrast, the less crowded coordination sphere around Li2 allows for a closer approach to the Cp ring (Li2–Cp1 = 1.866 Å; Li2–C = 2.18(2)–2.28(2) Å). Within the unit presented in Fig. 3, there is an almost linear O–Li–Cp_{centroid}–Li–Cp_{centroid} linkage (O1–Li2–Cp1 = 177.49°; Li2–Cp1–Li1 = 176.79°; Cp1–Li1–Cp1* = 180.00°), although the disordered lithium results in an overall zig-zag pattern.

Colorless crystals of **3a** were obtained by cooling a saturated THF/TMEDA (TMEDA = *N,N,N',N'*-tetramethylethylenediamine) solution of **2a** to –30 °C. A thermal ellipsoid diagram is shown in Fig. 5 with important bond lengths and angles presented in Table 3. The solid state structure reveals a discrete “triple ion” or metallate structure (see later), with a $[(\text{CpAr}^\#)_2\text{Li}]^-$ anion and a $[\text{Li}(\text{TMEDA})_2]^+$ cation. Only one of two independent molecules of each is shown; since the metric parameters are similar in both, the bond angles and lengths of only one will be discussed. Also, the two cyclopentadienyl rings within each $[(\text{CpAr}^\#)_2\text{Li}]^-$ unit are related by symmetry, and thus Table 3 contains only bond lengths between the lithium center and one of the Cp groups. Although alkali metal cyclo-

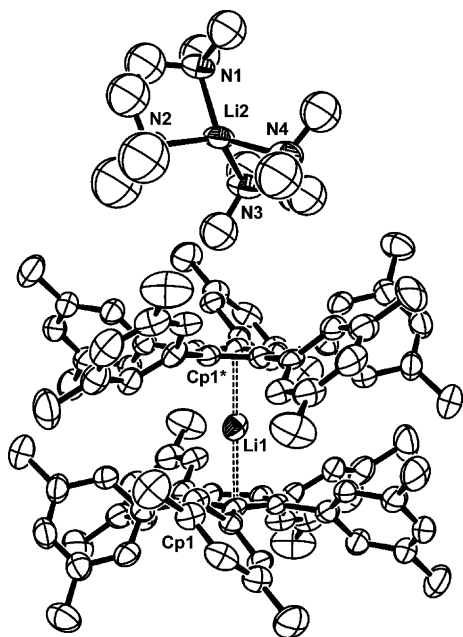


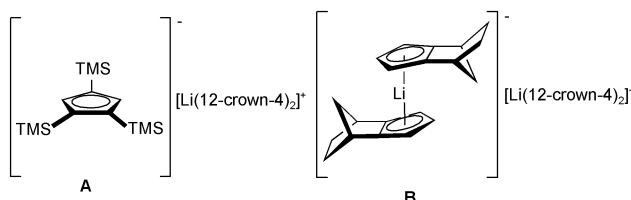
Fig. 5 Thermal ellipsoid view of $[(\text{CpAr}^\#)_2\text{Li}][\text{Li}(\text{TMEDA})_2]$ (**3a**) ($\text{Ar}^\# = 3,5\text{-Me}_2\text{C}_6\text{H}_3$) drawn with 30% probability ellipsoids, giving the atom numbering scheme used in the tables. Only one of two independent molecules is shown. Cp1 is defined as the centroid arising from atoms C1–C5; Cp1* is defined as the centroid arising from atoms C1*–C5*. For the sake of clarity, only the centroid designations are given.

Table 3 Selected bond distances (Å) and angles (°) for $[(\text{CpAr}^\#)_2\text{Li}][\text{Li}(\text{TMEDA})_2]$ (**3a**) ($\text{Ar}^\# = 3,5\text{-Me}_2\text{C}_6\text{H}_3$)^a

Li1–Cp1	2.086	Li1–C1	2.445(4)
Li1–C2	2.441(4)	Li1–C3	2.405(4)
Li1–C4	2.377(4)	Li1–C5	2.400(4)
Li2–N1	2.080(9)	Li2–N2	2.103(10)
Li2–N3	2.169(11)	Li2–N4	2.112(10)
Cp1–Li1–Cp1*	180.00	N1–Li1–N2	88.2(4)
N1–Li1–N3	124.5(5)	N1–Li1–N4	120.6(5)
N2–Li1–N3	118.5(4)	N2–Li1–N4	122.6(5)
N3–Li1–N4	86.5(4)		

^a Cp1 is defined as the centroid arising from atoms C1 – C5; Cp1* is related to Cp1 by symmetry.

pentadienide complexes commonly reveal ionic polymeric chain structures, as observed for **2a**, solvation of the metal cation can break the chain into smaller units. The use of crown ethers can result in cation–anion separation and the formation of cyclopentadienide anions, as observed in $[(1,2,4\text{-tris}(\text{trimethylsilyl})\text{cyclopentadienide})][\text{Li}(12\text{-crown-4})]$ (A),²⁰ or so-called “triple ions”, obtained by the specific solvation of only half of the lithium cations. To date, the only cyclopentadienyl derivative to exhibit this structural motif is the isodicyclopentadienide species $[(\text{isodiCp})_2\text{Li}][\text{Li}(12\text{-crown-4})]$ (B),¹¹ although related porphyrin²¹ and carborane²² complexes have been reported.



The formation of the triple ion **3a** upon addition of TMEDA to a THF solution of **2a** differs from the pattern of reactivity seen for lithium isodicyclopentadienide.¹¹ In solution, the THF solvated triple ion $[(\text{isodiCp})_2\text{Li}][\text{Li}(\text{THF})_4]$ is postulated to exist in equilibrium with the monomer, $(\text{isodiCp})\text{Li}(\text{THF})_x$. Addition of TMEDA to an ethereal solution of $(\text{isodiCp})\text{Li}$ yields $(\text{isodiCp})\text{Li}(\text{TMEDA})$. The triple ion B is only obtained upon treating an equilibrium mixture of $(\text{isodiCp})\text{Li}(\text{THF})_x$ and $[(\text{isodiCp})_2\text{Li}][\text{Li}(\text{THF})_4]$ with an excess of 12-crown-4. This difference in observed reactivity with Lewis bases is due to the increased steric demands of the penta-arylated cyclopentadienyl ligand.

As observed in **2a**, the two Cp rings are planar (Cp1–Li1–Cp1* = 180.00°) and the lithium ion is only loosely held between the two. The Li1–centroid distance of 2.086 Å is essentially the same as that determined for **2a** (Li1–C = 2.377(4)–2.445(4) Å) and longer than those in $[(\text{isodiCp})_2\text{Li}][\text{Li}(12\text{-crown-4})]$ (1.987 and 2.008 Å).¹¹ Again, the Li–Cp distance is determined by the steric encumbrance of the 3,5-Me₂C₆H₃ rings, which prevents the rings from any closer approach. The phenyl rings are canted an average of 47.7° and have the same opposing orientation that was seen in **2a**. The bond lengths and angles within the $[\text{Li}(\text{TMEDA})_2]^+$ cation are unremarkable and similar to those previously reported for related compounds.^{11,22–24}

^7Li NMR spectroscopy and solution equilibria

The solid-state structures of **2a** and **3a** indicated that solvation is important in these complexes, and generates different structural types depending on the Lewis base employed. We were interested in whether such structures were also present in solution. To further elucidate the nature of “ $(\text{CpAr}^\#)_2\text{Li}(\text{solvent})_x$ ” in solution, we turned to ^7Li NMR spectroscopy. The room temperature ^7Li NMR spectrum of $\{[(\text{CpAr}^\#)_2\text{Li}][\text{Li}(\text{THF})]_x(\text{THF})\}_x$ (**2a**) in C_6D_6 is shown in Fig. 6. The spectrum consists of three distinct singlets at -0.21 , -0.86 and -1.96 ppm of intensity 4 : 1 : 1. These three peaks correspond to two separate lithium-containing species: the monomer $(\text{CpAr}^\#)_2\text{Li}(\text{THF})_x$ (-0.21 ppm) and the solvent-separated ion pair, $[(\text{CpAr}^\#)_2\text{Li}][\text{Li}(\text{THF})_x]$ (-0.86 ppm, THF-solvated lithium; -1.96 ppm, “sandwiched” lithium), which are in equilibrium at room temperature [eqn. (4)]. Such monomer–dimer equilibria have been observed for CpLi and substituted cyclopentadienyl lithium salts in d^8 -THF below -100 °C,^{10,25,26} the dynamic exchange process is slowed considerably by the grafting of five 3,5- $\text{Me}_2\text{C}_6\text{H}_3$ moieties onto the Cp ring. There also appears to be little effect of temperature (20 to -85 °C) on the relative ratios of the two species in solution (2 monomer : 1 dimer). A similar example of a temperature independent equilibrium was noted for CCpLi (CCp = camphor-cyclopentadienyl) in THF between -100 °C and room temperature.²⁵ The chemical shifts of the two Cp-containing compounds are in the normal range for lithium chemical shifts (*ca.* $+2$ to -2 ppm). This contrasts with that reported for CpLi and other substituted lithium cyclopentadienides, for which resonances at -7.64 (CpLi monomer) and -12.78 ppm ($[(\text{Cp})_2\text{Li}]^-$ sandwich) were found. These anomalously large upfield shifts were ascribed to magnetic anisotropy and ring current effects. In the case of **2a**, the lithium centers must reside in much more traditionally shielded positions within the molecule.

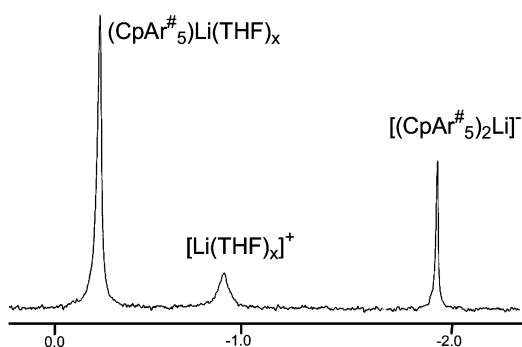


Fig. 6 194 MHz ^7Li NMR spectrum of $\{[(\text{CpAr}^\#)_2\text{Li}][\text{Li}(\text{THF})]_x(\text{THF})\}_x$ (**2a**) ($\text{Ar}^\# = 3,5\text{-Me}_2\text{C}_6\text{H}_3$) in C_6D_6 at room temperature.

Raising the temperature to 60 °C results in a single broad resonance at -0.50 ppm, consistent with rapid lithium exchange between compounds. This was confirmed by the ^7Li NOESY spectrum (Fig. 7), in which cross-peaks were found for the resonances arising from the monomer $(\text{CpAr}^\#)_2\text{Li}(\text{THF})_x$ (-0.21 ppm) and the sandwiched lithium center in $[(\text{CpAr}^\#)_2\text{Li}]^-$ (-1.96 ppm). At the mixing time employed ($t_{\text{mix}} = 500$ ms), no cross peak was present between the monomer $(\text{CpAr}^\#)_2\text{Li}(\text{THF})_x$ and $[\text{Li}(\text{THF})_x]^+$ (-0.86 ppm), although if the lithium center in $(\text{CpAr}^\#)_2\text{Li}(\text{THF})_x$ is exchanging with

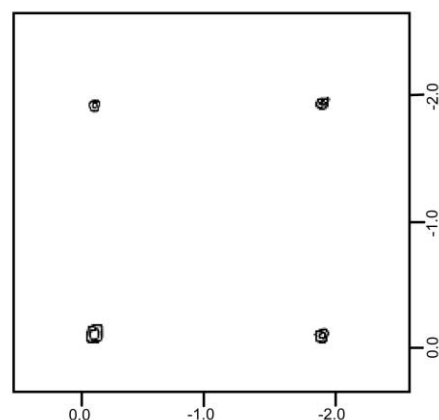
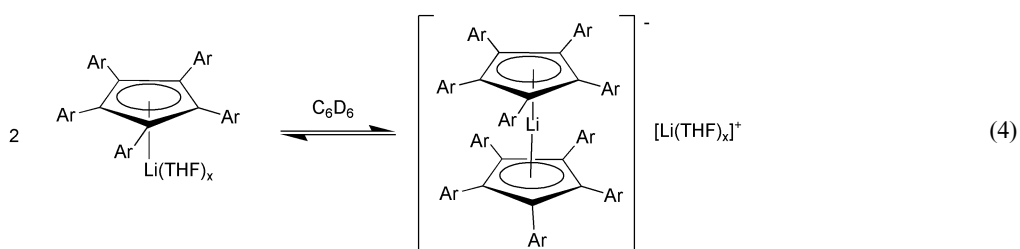


Fig. 7 194 MHz ^7Li NOESY spectrum of $\{[(\text{CpAr}^\#)_2\text{Li}][\text{Li}(\text{THF})]_x(\text{THF})\}_x$ (**2a**) ($\text{Ar}^\# = 3,5\text{-Me}_2\text{C}_6\text{H}_3$) in C_6D_6 at room temperature.

$[(\text{CpAr}^\#)_2\text{Li}]^-$, it must also be exchanging with the THF solvated cation. Changing the mixing time to 25 ms resulted in the appearance of the resonance arising from $[\text{Li}(\text{THF})_x]^+$ on the diagonal, but still no cross-peaks were observed. This must be due to an additional exchange process such as THF dissociation in $[\text{Li}(\text{THF})_x]^+$ that relaxes the lithium atom to such an extent that intermolecular exchange with this metal center is not observed under these measurement conditions.

In d^8 -THF, the ^7Li NMR spectrum exhibits two peaks of equal intensity at 4.24 and -2.80 ppm at room temperature. Heating the sample to 60 °C does not lead to any significant change in the spectrum, suggesting that there is no exchange between lithium sites. This was confirmed by ^7Li NOESY experiments, where no cross peaks were observed ($t_{\text{mix}} = 25$ to 500 ms). These data are consistent with the solvent-separated ion pair, $[(\text{CpAr}^\#)_2\text{Li}][\text{Li}(\text{THF})_x]$ in THF solution. The lack of lithium exchange in this species is supported by the absence of cross peaks between the resonances due to $[\text{Li}(\text{THF})_x]^+$ (-0.86 ppm) and $[(\text{CpAr}^\#)_2\text{Li}]^-$ (-1.96 ppm) when the spectrum was taken in C_6D_6 (Fig. 6). Titration of a C_6D_6 solution of **2a** with THF resulted in numerous additional signals until the final spectrum observed in d^8 -THF was obtained. This suggests that the situation is more complex in coordinating solvents, possibly involving dimeric species, close-ion pairs, solvent-separated ion pairs, super sandwiches or other more exotic structures. Previous MNDO calculations on related systems postulate that a super sandwich structure $[(\text{Cp})\text{Li}(\text{Cp})\text{Li}(\text{solvent})_x]$ (Fig. 3) is more stable than a solvent-separated ion pair $[(\text{Cp})_2\text{Li}][\text{Li}(\text{TMEDA})_2]$ (Fig. 5) and may play a large part in describing the solution dynamics of such systems.²⁶ Paquette *et al.* have shown that many unusual structures may exist in equilibrium in solution.^{10,25,26}

The ^7Li NMR spectrum of $[(\text{CpAr}^\#)_2\text{Li}][\text{Li}(\text{TMEDA})_2]$ (**3a**) in C_6D_6 consists of a single sharp resonance at 6.80 ppm which does not change upon cooling (C_7D_8). This suggests either (a) fast exchange on the NMR timescale between a monomer such as $(\text{CpAr}^\#)_2\text{Li}(\text{TMEDA})$ and the solvent separated ion pair, $[(\text{CpAr}^\#)_2\text{Li}][\text{Li}(\text{TMEDA})_2]$ or (b) the presence of a single static structure in solution. The ^7Li NMR chemical shift supports the latter, as the presence of only one $\text{CpAr}^\#$ ring would result in a downfield shift relative to the sandwich complex. It is possible for a structure such as that observed for **3a** to exist



without participating in an equilibrium with a solvated monomer; the ^7Li NMR spectrum of the lithiacarborane complex $[1,1'-\text{Li}\{2,3-(\text{SiMe}_3)_2-2,3-\text{C}_2\text{B}_4\text{H}_5\}_2][\text{Li}(\text{TMEDA})_2]$ exhibits two distinct peaks, consistent with a single solution structure which is the same as that determined in the solid state.²² We suggest that in solution the formulation $(\text{CpAr}^{\#}_5)\text{Li}(\text{TMEDA})$ is most likely, as found for $(\text{isodiCp})\text{Li}(\text{TMEDA})$, although only a small reorganization energy must be necessary to form the triple ion observed in the solid state. This is supported by the ^{13}C NMR spectrum of **3a**, which is comprised of multiple resonances, consistent with a more complex solution behavior.

The ^7Li NMR spectrum of **2b** consisted of two peaks of roughly equal intensity at 1.18 and -4.43 ppm; the downfield resonance was significantly broadened ($\Delta_{1/2} = 120$ Hz) as compared to the upfield resonance ($\Delta_{1/2} = 5$ Hz). The presence of two peaks points towards a monomer/dimer equilibrium in solution. Recent studies on lithium pentabenzylcyclopentadienides have revealed that bulky systems such as those employed here often favor arene complexes over polymers commonly observed with smaller cyclopentadienyl groups. Schnöckel *et al.* have postulated that small neutral arene adducts such as $[\{\text{Li}(\eta^5\text{-CpR}_5)\}_2(\text{C}_6\text{D}_6)]$ may be formed when (1) R is bulky enough to prevent polymer formation, (2) no proper cation can be generated and (3) no donor solvent is present.¹⁹ The ^7Li NMR spectrum of $\text{Li}(\eta^5\text{-C}_5\text{Bz}_5)$ ($\text{Bz} = \text{CH}_2\text{C}_6\text{H}_5$) in C_6D_6 revealed a single resonance, indicating either the presence of a monomeric species, or a fast equilibrium between monomeric and dimeric species. The presence of two peaks in the ^7Li NMR spectrum of **2b** may be attributed to the larger size of the di-*tert*-butylphenyl groups, which slows down the exchange and allows for both species to be observed. The broadened peak at 1.18 ppm is likely due to the more unsymmetric environment about the lithium atom in the monomer $(\text{CpAr}^{\#}_5)\text{Li}$, while the sharper peak may be the result of a more highly symmetric species such as a dimer $[\{(\text{CpAr}^{\#}_5)\text{Li}\}_2(\text{C}_6\text{D}_6)]$ or higher oligomer $\{(\text{CpAr}^{\#}_5)\text{Li}\}_x$. We should also note that the assignment of the upfield resonance to a dimeric species is somewhat speculative since we were unable to obtain a solid state structure for **2b** *i.e.* a dimeric, trimeric or higher order aggregate is possible. It should also be noted that although two species were evident in the ^7Li NMR spectrum of **2b**, only a single set of resonances was observed in the ^1H and ^{13}C NMR spectra. This may be due to the different frequencies of ^7Li , ^{13}C and ^1H NMR spectroscopy, resulting in the observation of averaged signals when observing one nucleus but distinct species for another. Also, the protons observed in these complexes are quite far removed from the metal center, and thus the difference in chemical shift between monomeric and oligomeric products may be negligible.

Conclusions

The superbuly cyclopentadienes, CpAr_5H , are readily deprotonated by BuLi to give lithium salts of the general formula $(\text{CpAr}_5)\text{Li}(\text{solvent})_x$; the solution behavior observed is similar to that reported for other bulky Cp derivatives such as lithium isodicyclopentadienide. The large aryl groups in **2a** slow down the exchange between $(\text{CpAr}^{\#}_5)\text{Li}(\text{THF})_x$ and $[(\text{CpAr}^{\#}_5)_2\text{Li}][\text{Li}(\text{THF})_x]$ such that all three distinct lithium environments can be observed under ambient conditions. The crystal structures of **2a** and **3a** further lend credence to the proposed solution structures although the presence of further more complicated structures in solution cannot be discounted.

Experimental

General considerations

All manipulations were carried out under an inert atmosphere of oxygen-free UHP grade argon using standard Schlenk

techniques or under oxygen-free helium in a Vacuum Atmospheres glovebox. Cp_2ZrCl_2 and dimethylformamide (<30 ppm H_2O) were purchased from Strem Chemical Co. and used as received. 3,5-dimethyl-1-bromobenzene was obtained from Lancaster and dried over molecular sieves prior to use. 3,5-di-*t*-butyl-1-bromobenzene was obtained from Lancaster and used as received. Caesium carbonate, tri-*t*-butyl-phosphine, *p*-toluenesulfonic acid, sodium carbonate, sodium chloride, magnesium sulfate, palladium acetate and BuLi were purchased from Aldrich and used as received. Methylene chloride and chloroform were purchased from Fisher and used as received. *N,N,N',N'*-tetramethylethylenediamine was purchased from Aldrich and distilled over sodium prior to use. Hexanes, toluene, diethyl ether and tetrahydrofuran were de-oxygenated by passage through a column of supported copper redox catalyst (Cu-0226 S) and dried by passing through a second column of activated alumina.²⁷ C_6D_6 and d^8 -THF were dried over Na–K alloy, trap-to-trap distilled and degassed before use. ^1H , $^{13}\text{C}\{^1\text{H}\}$ and $^7\text{Li}\{^1\text{H}\}$ spectroscopy were performed at ambient temperature on a Bruker DRX-500 spectrometer operating at 500.0, 125.1 and 194.4 MHz respectively. ^1H chemical shifts are given relative to residual $\text{C}_6\text{D}_5\text{H}$ ($\delta = 7.15$ ppm) or $\text{C}_4\text{D}_7\text{HO}$ ($\delta = 3.58$ ppm). ^{13}C chemical shifts are given relative to C_6D_6 ($\delta = 128.39$ ppm). ^7Li chemical shifts are given relative to external LiCl in D_2O ($\delta = 0.0$ ppm). The ^7Li NOESY spectrum was obtained on a Bruker DRX-500 spectrometer operating at 194.4 MHz in C_6D_6 at 283 K; t_1 was incremented in 512 steps, and the data were zero-filled to 1024 words before Fourier transformation. Sixteen scans were recorded for each increment with $t_{\text{mix}} = 500$ or 25 ms with a relaxation time of 800 ms. Infrared spectra were recorded on a Nicolet Avatar 360 FT-IR spectrometer; solid-state spectra were taken as Nujol mulls between KBr plates. Elemental analyses were performed by the Micro-Mass Facility at the University of California, Berkeley.

(CpAr₅)H (**Ar** = 3,5-Me₂C₆H₃, **1a**; 3,5-Bu₂C₆H₃, **1b**). This compound was prepared by a modification of the original literature procedure⁵ as reported to us by Fu *et al.*²⁸ For **1a**: In the glovebox, Cp_2ZrCl_2 (584 mg, 2.00 mmol), 3,5-dimethyl-1-bromobenzene (4.44 g, 24.0 mmol), caesium carbonate (7.82 g, 24.0 mmol), palladium acetate (112 mg, 0.500 mmol), tri-*t*-butylphosphine (404 mg, 2.00 mmol) and 50 mL DMF were combined in a Schlenk tube. The contents were then heated to 130 °C in an oil bath for 24 h, forming a creamy brown slurry. The Schlenk tube and its contents were then cooled to room temperature and exposed to air. 150 mL CH_2Cl_2 was then added, followed by *p*-toluenesulfonic acid (9.12 g, 48.0 mmol). This was stirred at room temperature for 15 min, then passed through a column of silica gel to yield a brown solution. The column was additionally rinsed with small portions of CH_2Cl_2 and DMF until the washings were colorless (~ 10 mL each). The solvent was then removed under vacuum to give a brown tar. The solid was dissolved in CHCl_3 (150 mL) and extracted with saturated aqueous NaHCO_3 solution (3×150 mL) and saturated aqueous NaCl solution (3×150 mL). The organic layer was dried over MgSO_4 and passed through a column of silica gel to give a brown solution. The solvent was removed under vacuum and the oily solid washed with hexanes until the washings were colorless, yielding **1a** as a yellow–orange solid (1.54 g, 66% yield). The *t*-butyl derivative **1b** was prepared in a similar fashion from 3,5-di-*t*-butyl-1-bromobenzene (3.14 g, 78% yield). For **1a**: analytical data for this compound have been reported previously.⁵ For **1b**: ^1H NMR (C_6D_6): δ 7.41 (br d, $^4J_{\text{H-H}} = 1.5$ Hz, 2H, *o*-H), 7.29 (br t, $^4J_{\text{H-H}} = 1.5$ Hz, 1H, *p*-H), 7.27 and 7.23 (br t, $^4J_{\text{H-H}} = 1.5$ Hz, 2H, *p*-H), 7.18 and 7.13 (br d, $^4J_{\text{H-H}} = 1.5$ Hz, 4H, *o*-H), 5.24 (s, 1H, CpH), 1.28 (s, 18H, *t*-Bu–Ph) 1.16 and 1.15 (s, 36H, *t*-Bu–Ph). $^{13}\text{C}\{^1\text{H}\}$ NMR (C_6D_6): δ 151.23, 150.80, 150.10, 148.15, 146.06, 139.01, 137.42, 136.60, 125.27, 124.67, 123.76, 120.86, 120.32, 120.16, 63.81, 35.27, 35.07, 32.95, 32.38, 31.97, 31.54. IR (Nujol, cm^{-1}): 1592 (s), 1362 (m), 1248

Table 4 Crystallographic data^a

Compound	1a	2a	3a
Formula	C ₄₅ H ₄₆	C ₉₈ H ₁₀₆ Li ₂ O ₂	C ₁₁₀ H ₁₃₈ Li ₂ N ₄ O ₂
MW	586.82	1329.71	1562.18
Crystal system	triclinic	triclinic	triclinic
Space group	<i>P</i> $\bar{1}$	<i>P</i> $\bar{1}$	<i>P</i> $\bar{1}$
Temp/K	203	203	203
<i>a</i> /Å	8.1689(19)	13.997(4)	14.216(4)
<i>b</i> /Å	12.805(3)	15.486(4)	20.023(5)
<i>c</i> /Å	17.290(4)	20.198(5)	22.771(6)
<i>a</i> ^o	92.202(4)	97.393(4)	98.140(6)
<i>β</i> ^o	93.823(5)	102.993(5)	106.914(4)
<i>γ</i> ^o	104.869(5)	96.523(4)	109.938(5)
<i>V</i> /Å ³	1741.3(7)	4184.2(18)	5617(3)
<i>Z</i>	2	2	2
<i>μ</i> /mm ⁻¹	0.063	0.060	0.056
Reflections	8242	20273	28915
Independent reflections	4694	10298	13878
<i>R</i> _{int}	0.0266	0.0413	0.0454
<i>R</i> ₁	0.0669	0.0933	0.0962
<i>wR</i> ₂	0.2181	0.2534	0.2744

^a $R_1 = \sum ||F_o| - |F_c|| / \sum |F_o|$ and $wR_2 = [\sum (\omega(F_o^2 - F_c^2)^2) / \sum (\omega(F_o^2))]^{1/2}$; $\omega = 1 / [\sigma^2(F_o^2) + (aP)^2]$, where $a = 0.1350, 0.1284$ and 0.1776 .

(m), 1201 (w), 1018 (w), 910 (w), 872 (w), 711 (m). Anal. Calcd. for C₇₈H₁₁₃NO [1b(DMF)]: C, 86.68; H, 10.54%. Found: C, 86.52; H, 10.82%.

{[(CpAr[#])₅Li][Li(THF)](THF)}_x (2a) (Ar[#] = 3,5-Me₂C₆H₃).

ⁿBuLi (0.39 mL of a 1.6 M hexane solution, 0.62 mmol) was added dropwise to an orange solution of **1a** (330 mg, 0.57 mmol) in 10 ml THF, causing a precipitate to form. This was stirred for 15 min and the solvent was then removed under vacuum. The yellow–orange solid was washed with toluene, collected on a frit and dried under vacuum (290 mg, 68% yield). Slow evaporation of a saturated toluene solution yielded large colorless crystals of **2a**. ¹H NMR (C₆D₆): δ 6.95 (br s, 10H, *o*-H), 6.69 (br s, 5H, *p*-H), 3.42 (m, 8H, THF), 2.06 (s, 30H, *Me*Ph), 1.28 (m, 8H, THF). ¹³C{¹H} NMR (C₆D₆): the spectrum of **2a** was complicated by the presence of many species in solution. ⁷Li{¹H} NMR (C₆D₆, 20 °C): δ -0.21 ((CpAr[#])₅Li(THF)_x), -0.86 ([Li(THF)_x]⁺), -1.96 ([CpAr[#])₅-Li]⁻); (C₆D₆, 60 °C): δ -0.50; (d⁸-THF, 20 °C): δ 4.24, -2.80. IR (Nujol, cm⁻¹): 1592 (s), 1300 (w), 1033 (s), 947 (w), 908 (m), 893 (m), 840 (s), 761 (m), 725 (m), 708 (m), 692 (m), 680 (m). Anal. Calcd. for C₁₀₂H₁₁₄Li₂O₃: C, 87.39; H, 8.20%. Found: C, 87.20; H, 8.30%.

(CpAr^{*})₅Li (2b) (Ar^{*} = 3,5-^tBu₂C₆H₃). ⁿBuLi (0.13 mL of a 1.6 M hexane solution, 0.20 mmol) was added dropwise to an orange solution of **1b** (200 mg, 0.20 mmol) in 10 ml diethyl ether, causing the solution to lighten slightly. This was stirred for 3 h and the solution was then cooled to -30 °C, yielding **2b** as small colorless crystals (160 mg, 80% yield). ¹H NMR (C₆D₆): δ 7.19 (br t, ⁴J_{H-H} = 1.5 Hz, 5H, *p*-H), 7.01 (br d, ⁴J_{H-H} = 1.5 Hz, 10H, *o*-H), 1.19 (s, 90H, *t*-Bu-Ph). ¹³C{¹H} NMR (C₆D₆): δ 149.82, 139.07, 126.37, 120.80, 117.65, 34.98, 32.05. ⁷Li{¹H} NMR (C₆D₆): δ 1.18, -4.43. IR (Nujol, cm⁻¹): 1591 (s), 1303 (m), 1248 (m), 1201 (w), 1168 (w), 1152 (w), 1058 (w), 1017 (m), 967 (w), 894 (m), 870 (m), 842 (w), 775 (w), 722 (s). Anal. Calcd. for C₇₅H₁₀₅Li: C, 88.87; H, 10.44%. Found: C, 86.27; H, 11.05%.

{[(CpAr[#])₅Li][Li(TMEDA)]₂} (3a) (Ar[#] = 3,5-Me₂C₆H₃). **2a** (250 mg, 0.43 mmol) was dissolved in THF with heating and TMEDA (0.5 mL) was added. The solution was cooled to -30 °C, resulting in large colorless crystals (310 mg, 90% yield). ¹H NMR (C₆D₆): δ 6.95 (br s, 20H, *o*-H), 6.68 (br s, 10H, *p*-H), 2.31 (s, 8H, TMEDA), 2.12 (s, 24H, TMEDA), 2.08 (s, 60H, *Me*Ph). ¹³C{¹H} NMR (C₆D₆): the spectrum of **3a** was complicated by the presence of many species in solution. ⁷Li{¹H} NMR (C₆D₆):

δ 6.80. IR (Nujol, cm⁻¹): 1598 (s), 1351 (w), 1302 (w), 1168 (w), 1082 (w), 1033 (m), 909 (w), 897 (w), 850 (s), 841 (s), 775 (w), 754 (w), 725 (m), 704 (m), 692 (s). Anal. Calcd. for C₉₀H₉₀Li₂ [3a - 2(TMEDA)]: C, 91.18; H, 7.65%. Found: C, 91.98; H, 8.13%.

Crystallographic studies

The crystal structures of all compounds were determined as follows, with exceptions noted in subsequent paragraphs: a crystal was mounted onto a glass fiber using a spot of silicone grease. Due to air sensitivity, the crystal was mounted from a pool of mineral oil under argon gas flow. The crystal was placed on a Bruker P4/CCD diffractometer, and cooled to 203 K using a Bruker LT-2 temperature device. The instrument was equipped with a sealed, graphite monochromatized MoK α X-ray source ($\lambda = 0.71073$ Å). A hemisphere of data was collected using φ scans, with 30 s frame exposures and 0.3° frame widths. Data collection and initial indexing and cell refinement were handled using SMART²⁹ software. Frame integration, including Lorentz-polarization corrections, and final cell parameter calculations were carried out using SAINT³⁰ software. The data were corrected for absorption using the SADABS³¹ program. Decay of reflection intensity was monitored *via* analysis of redundant frames. The structure was solved using direct methods and difference Fourier techniques. All hydrogen atom positions were idealized, and rode on the atom they were attached to. The final refinement included anisotropic temperature factors on all non-hydrogen atoms. Structure solution, refinement, graphics, and creation of publication materials were performed using SHELXTL NT.³² Additional details of data collection and structure refinement are listed in Table 4.

(CpAr[#])₅H (1a). the unique hydrogen atom position was located on the difference map, and refined with isotropic temperature factor set to 0.08 Å².

{[(CpAr[#])₅Li][Li(THF)](THF)}_x (2a). the electron density of a disordered THF molecule was refined with the aid of PLATON/SQUEEZE³³ (74 e⁻ cell⁻¹ and 838 Å³).

[(CpAr[#])₅Li][Li(TMEDA)]₂ (3a). the electron density of a disordered THF molecule was refined with the aid of PLATON/SQUEEZE³³ (209 e⁻ cell⁻¹ and 1728 Å³).

CCDC reference numbers 200149–200151.

See <http://www.rsc.org/suppdata/dt/b3/b302258g/> for crystallographic data in CIF or other electronic format.

Acknowledgements

We thank the research group of Dr. Greg Fu (MIT) for helpful discussions regarding the isolation of compounds **1a** and **1b**, and Dr. Kevin D. John (LANL) for acquiring the X-ray data for compound **1a**. This work was performed under the auspices of the Laboratory Directed Research and Development Program. Los Alamos National Laboratory is operated by the University of California for the U.S. Department of Energy under Contract W-7405-ENG-36.

References

- 1 P. Jutzi and N. Burford, *Chem. Rev.*, 1999, **99**, 969.
- 2 C. Janiak and H. Schumann, *Adv. Organomet. Chem.*, 1991, **33**, 291.
- 3 J. Okuda, *Top. Curr. Chem.*, 1992, **160**, 97.
- 4 M. Miura, S. Pivsa-Art, G. Dyker, J. Heiermann, T. Satoh and M. Nomura, *Chem. Commun.*, 1998, 1889.
- 5 G. Dyker, J. Heiermann, M. Miura, J. I. Inoh, S. Pivsa-Art, T. Satoh and M. Nomura, *Chem. Eur. J.*, 2000, **6**, 3426.
- 6 B. Tao, M. M. C. Lo and G. C. Fu, *J. Am. Chem. Soc.*, 2001, **123**, 353.
- 7 D. Seebach, *Angew. Chem., Int. Ed. Eng.*, 1988, **27**, 1624.
- 8 D. B. Collum, *Acc. Chem. Res.*, 1993, **26**, 227.
- 9 B. L. Lucht and D. B. Collum, *Acc. Chem. Res.*, 1999, **32**, 1035.
- 10 L. A. Paquette, W. Bauer, M. R. Sivik, M. Buhl, M. Feigel and P. von Rague Schleyer, *J. Am. Chem. Soc.*, 1990, **112**, 8776.
- 11 F. Zaegel, J. C. Gallucci, P. Meunier, B. Gautheron, M. R. Sivik and L. A. Paquette, *J. Am. Chem. Soc.*, 1994, **116**, 6466.
- 12 L. D. Field, T. W. Hambley, C. M. Lindall and A. F. Masters, *Inorg. Chem.*, 1992, **31**, 2366.
- 13 P. G. Evard, P. Piret, G. Germain and M. V. Meerssche, *Acta Crystallogr., Sect. B*, 1971, **27**, 661.
- 14 C. Janiak, R. Weimann and F. Gorlitz, *Organometallics*, 1997, **16**, 4933.
- 15 R. E. Dinnebier, U. Behrens and F. Olbrich, *Organometallics*, 1997, **16**, 3855.
- 16 M. J. Harvey, T. P. Hanusa and M. Pink, *J. Chem. Soc., Dalton Trans.*, 2001, 1128.
- 17 W. J. Evans, J. C. Brady, C. H. Fujimoto, D. G. Giarikos and J. W. Ziller, *J. Organomet. Chem.*, 2002, **649**, 252.
- 18 M. L. Cole, C. Jones and P. C. Junk, *J. Chem. Soc., Dalton Trans.*, 2002, 896.
- 19 C. Dohmeier, E. Baum, A. Ecker, R. Koppe and H. Schnockel, *Organometallics*, 1996, **15**, 4702.
- 20 H. Chen, P. Jutzi, W. Leffers, M. M. Olmstead and P. P. Power, *Organometallics*, 1991, **10**, 1282.
- 21 J. Arnold, *J. Chem. Soc., Chem. Commun.*, 1990, 976.
- 22 N. S. Hosmane, J. Yang, H. Zhang and J. A. Maguire, *J. Am. Chem. Soc.*, 1996, **118**, 5150.
- 23 M. F. Lappert, A. Singh, L. M. Engelhardt and A. H. White, *J. Organomet. Chem.*, 1984, **262**, 271.
- 24 A. Hammel, W. Schwarz and J. Weidlin, *Acta Crystallogr., Sect. C*, 1990, **46**, 2337.
- 25 W. Bauer, G. O'Doherty, P. von Rague Schleyer and L. A. Paquette, *J. Am. Chem. Soc.*, 1991, **113**, 7093.
- 26 W. Bauer, M. R. Sivik, D. Friedrich, P. von Rague Schleyer and L. A. Paquette, *Organometallics*, 1992, **11**, 4178.
- 27 A. B. Pangborn, M. A. Giardello, R. H. Grubbs, R. K. Rosen and F. J. Timmers, *Organometallics*, 1996, **15**, 1518.
- 28 B. Tao and G. C. Fu, personal communication.
- 29 G. M. Sheldrick, *SMART Version 4.210*, Bruker Analytical X-ray Systems, Madison, WI, 1996.
- 30 G. M. Sheldrick, *SAINTE Version 5.050*, Bruker Analytical X-ray Systems, Madison, WI, 1998.
- 31 G. M. Sheldrick, *SADABS, Program for area detector adsorption correction*, Institute for Inorganic Chemistry, University of Göttingen, Germany, first release, 1996.
- 32 SHELXTL NT Version 5.10, Bruker Analytical X-ray Instruments, Madison, WI, 1997.
- 33 A. L. Spek, *Acta Crystallogr., Sect. A*, 1990, **46**, C34.